The antioxidant effects of butylated hydroxytoluene on cryopreserved goat sperm from a proteomic perspective

Chunyan Li[1,2,3], Larbi Allai[1,4], Jiachong Liang[1,2,3], Chunrong Lv[1,2,3], Xiaoqi Zhao[1,3], Xiaojun Ni[1,3], Guoquan Wu[1,2,3], Weidong Deng[5], Bouabid Badaoui[6] and Guobo Quan[1,2,3]

[1] Yunnan Animal Science and Veterinary Institute, Kunming, China
[2] Yunnan Provincial Genebank of Livestock and Poultry Genetic Resources, Kunming, China
[3] Yunnan Provincial Engineering Research Center of Animal Genetic Resource Conservation and Germplasm Enhancement, Kunming, China
[4] Higher School of Technology Sidi Bennour, Chouaib Doukkali University, El Jadida, Morocco
[5] School of Animal Science and Technology, Yunnan Agricultural University, Kunming, China
[6] Faculty of Sciences, Mohammed V University, Rabat, Morocco

ABSTRACT

At present, there are few reports about the proteomics changes provoked by butylated hydroxytoluene (BHT) supplementation on cryopreserved semen in mammals. Thus, we aimed to evaluate the effects of different concentrations of BHT on goat sperm and to investigate the proteomics changes of adding BHT to cryopreserved goat (*Capra hircus*) sperm. Firstly, semen samples were collected from four goats, and frozen in the basic extenders containing different concentrations of BHT (0.5 mM, 1.0 mM, 2.0 mM) and a control without BHT, respectively. After thawing, the protective effects of dose-dependent replenished BHT to the freezing medium on post-thaw sperm motility, integrities of plasma membrane and acrosome, reactive oxygen species levels were confirmed, with 0.5 mM BHT being the best (B group) as compared to the control (without BHT, C group). Afterwards, TMT-based quantitative proteomic technique was performed to profile proteome of the goat sperm between C group and B group. Parallel reaction monitoring was used to confirm reliability of the data. Overall, 2,476 proteins were identified and quantified *via* this approach. Comparing the C and B groups directly (C *vs.* B), there were 17 differentially abundant proteins (DAPs) potentially associated with sperm characteristics and functions were identified, wherein three were upregulated and 14 were downregulated, respectively. GO annotation analysis demonstrated the potential involvement of the identified DAPs in metabolic process, multi-organism process, reproduction, reproductive process, and cellular process. KEGG enrichment analysis further indicated their potential roles in renin-angiotensin system and glutathione metabolism pathways. Together, this novel study clearly shows that BHT can effectively improve quality parameters and fertility potential of post-thawed goat sperm at the optimal concentration, and its cryoprotection may be realized through regulation of sperm metabolism and antioxidative capability from the perspective of sperm proteomic modification.

Subjects Agricultural Science, Molecular Biology, Veterinary Medicine, Zoology
Keywords Semen, Cryopreservation, Sperm quality, Butylated hydroxytoluene, Proteome

INTRODUCTION

Semen cryopreservation is an important technology, which can preserve and utilize sperm for a long time, facilitating rapid dissemination of excellent genetic material around the world. Moreover, semen cryopreservation promotes the development and application of artificial insemination technology (AI), (*Leboeuf, Restall & Salamon, 2000*). However, the cryopreservation process has a deleterious impact on sperm normal physiology, reducing the quality because of adverse factors such as ultra-low temperature stress, osmotic stress and oxidative stress, ultimately, reducing the longevity and ability to fertilize such as vitality, acrosome reaction rate and egg fertilization rate (*Peris-Frau et al., 2020*).

Among these injuries caused by the cryopreservation process, oxidative lesion has been shown to greatly threaten sperm structures such as acrosome, mitochondria, nucleus DNA, and the functions such as motility and its ability to fusion with oocyte (*Pariz et al., 2019*). Given this, numerous antioxidants, previously reported, have been tested and added into freezing extenders to resist oxidative stress and improve fertility of post-thaw sperm (*Dutta, Majzoub & Agarwal, 2019*). In general, these antioxidants have been divided into two types: (1) enzymatic antioxidants, such as glutathione catalase (GSH-Px), glutathione reduction enzyme (GR), superoxide dismutase (SOD), glutathione-S-transferase (GST), melatonin, *etc*., (2) non-enzymatic antioxidants, such as glutathione (GSH), urate, vitamin, carbohydrate, *etc* (*Amidi et al., 2016*; *Jia et al., 2021*; *Riesco et al., 2021*; *Turk et al., 2022*; *Li et al., 2023*). Currently, many studies have been performed to assess the cryoprotective effects of these antioxidants on sperm during the cryopreservation process (*Pezo et al., 2021*; *Ribas-Maynou et al., 2021*; *Tiwari et al., 2022*).

Thereinto, butylated hydroxytoluene (BHT) is being investigated as a component to cryomedia in different animal species, including goat (*Memon et al., 2011*), human (*Merino et al., 2015*), boar (*Sus scrofa*) (*Trzcinska et al., 2015*), cat (*Jara et al., 2019*), and buffalo (*Nain et al., 2022*), because of its safety and notable anti-oxidative potential. BHT is a synthetic analogue of vitamin E, characterized with the low polarity and high lipid solubility (*Yehye et al., 2015*; *Achar et al., 2020*). It can be used to check auto-oxidation reaction of lipid bilayer and membrane by converting peroxy radicals into hydroperoxides, thus inhibiting lipid peroxidation (LPO). Besides, BHT also scavenges reactive oxygen species (ROS) from the surroundings of sperm, thereby minimizing the cold shock and increasing antioxidant defense of sperm during the cryopreservation process (*Merino et al., 2015*; *Khumran et al., 2019*). Although several studies have showed beneficial effects of BHT on sperm quality after cryopreservation, the specific cryoprotective mechanisms underlying have not been fully elucidated.

It is known that sperm is a specialized cell with inactive transcription, and therefore, once sperm has left the male reproductive tract, they rely mainly on the static population action of proteins and metabolites to maintain their function, prior to fertilization with oocytes, especially, the principal roles of proteins cannot be neglected (*Hermo et al., 2010*; *Chauvin et al., 2012*). Based on these facts that antioxidants play important roles in enhancement of frozen-thawed sperm antioxidative capability and the action mechanisms of most antioxidants remain unclear, taking BHT as an example, the aim of this study

endeavors to: (1) ascertain the optimal BHT concentration conducive to the preservation of post-thaw goat sperm quality, (2) elucidate the potential cryoprotective mechanism of this optimal BHT mainly from the perspective of goat sperm proteome. The identification of differential proteins coupled with their correlative bioinformatic analysis will deepen our understanding on the molecular mechanisms of BHT on mammalian sperm.

MATERIAL AND METHODS

Study design and workflow

The objective was to evaluate cryoprotective effects of different concentrations of BHT (0.0 mM, 0.5 mM, 1.0 mM, and 2.0 mM) on goat sperm during the cryopreservation process, indices related to sperm quality such as the motility, ROS levels, plasma membrane and acrosome integrities were assessed in current study. Thus, the optimal effect concentration of BHT was going to be determined. Afterwards, TMT-based quantitative proteomic technique was used to investigate potential effects of BHT on proteome of cryopreserved goat sperm. Overall workflow was shown in Fig. S1.

Semen preparation

During the whole experiment, the authors strictly complied with Regulations on the Administration of Laboratory Animals (Order-No.2 of the State Science and Technology Commission of the People's Republic of China, 1988) and Regulations on the Administration of Experimental Animals of Yunnan Province (the Standing Committee of Yunnan Provincial People's Congress 2007.10). All semen samples were acquired from Yi Xingheng Animal Science and Technology Co. Ltd (Kunming, Yunnan Province, China). Four males of Yunshang black goats with similar ages (2~3 years old) were selected, and kept in the same condition of feeding and management. Fresh semen (two ejaculates per male in 10 min) were collected *via* an artificial vagina method. Then, semen from each male was pooled and kept at 37 °C, and the quality was immediately assessed using a computer-assisted sperm analysis system (CASA, Microptic, Barcelona, Spain). Only semen meeting stringent quality criteria were accepted (volume of each semen ≥ 0.8 mL, sperm with concentration $\geq 2.5 \times 10^9$/mL, and the motility $\geq 80\%$) (*Liu et al., 2019*). Pooled semen from each male was subsequently divided into four aliquots. One was used as sperm source of cryopreserved control group (C group, which was diluted using medium A), while the remaining three were used as sperm sources of cryopreserved experiment groups (B groups, which were diluted using medium B, respectively).

Semen freezing medium

Above four semen aliquots of each male were lightly diluted with two types of frozen media (media A and B) at RT (25 ° C), until a final sperm concentration reached about 3×10^8 /mL, respectively (*Succu et al., 2011*). Medium A was made up of 254 mM Tris, 85 mM citric acid, 70 mM fructose, 1% (w/v) soybean lecithin, 6% (v/v) glycerin, 1×10^4 IU penicillin and 1×10^4 IU streptomycin. Medium B consisted of three subgroups being made up the medium A and three concentrations of butylated hydroxytoluene (BHT, Sigma-Aldrich, USA) with 0.5, 1.0 and 2.0 mM, respectively (*Merino et al., 2015*).

Freezing and thawing process

Extended semen samples were loaded into the labeled 0.25 mL straws (IMV technologies, L'Aigle, France), following by equilibration at 5 °C for 3 h. After that, freezing through being placed in liquid nitrogen vapor for 7 min (−80 °C), and directly into liquid nitrogen immediately for at least one week (*Ruiz-Diaz et al., 2020*). For the thawing process, frozen semen was thawed in water bath at 37 °C for 30 s (*Fang et al., 2019*; *Li et al., 2023*).

Evaluation of sperm-quality associated indices

Motilities of all post-thaw sperm from the C and B groups were assessed *via* the CASA system (*Amann & Waberski, 2014*). Plasma membrane integrity was assessed by the hypo-osmotic swelling test (HOST) with the GENMED kit (GMS14017, GENMED Scientifics Inc., Wilmington, MA, USA). Briefly, 10 µL of sperm sample was mixed with 100 µL of pre-heated hypo-osmotic solution, incubated at 37 °C for 30 min. 10 µL of the mixture was then smeared onto a pre-heated glass slide with a coverslip. Over 200 sperm were counted under a phase-contrast microscope (Axio Vert A1, Germany). Sperm with a coiled tail indicated its has intact plasma membrane. Integrity rate of sperm was calculated (*Zou et al., 2021*; *Li et al., 2023*). Additionally, acrosome integrity was evaluated by the fluorescein isothiocyanate labeled pea agglutinin (FITC-PSA) test, and the detailed method has been described in our previous report (*Jia et al., 2022*). For analysis of intracellular ROS production, 5 µL of post-thaw semen was diluted with 500 µL TALP solution, followed by 0.5 µL DCFH-DA and 5 µL PI for 60 min at 25 °C in darkness, the mixture was evaluated by a flow cytometer (BD Accuri™ C6, Franklin Lakes, NJ, USA) (*Najafi et al., 2018*).

TMT-based proteomic investigation
Sperm sample preparation

Post-thawing semen were centrifuged at 3,000× g for 15 min at 4 °C (JIDI-20RS, China). Collected sperm pellets were washed three times in 1× phosphate-buffered solution (1× PBS; Gibco, Thermo Scientific, Waltham, MS, USA) by centrifugation (3,000× g, 5 min, 4 °C), the pellet samples were immediately stored at −80 °C (*Zhu et al., 2020*).

Protein extraction and digestion

For protein extraction, every 30 mg sperm pellet was resuspended in the lysis buffer containing 8 M urea (Sigma, St. Louis, MO, USA), 2 mM EDTA (Sigma, St. Louis, MO, USA), 10 mM dithiothreitol (Sigma, St. Louis, MO, USA) and 1% protease inhibitor cocktail (SparkJade, Shandong, China), and incubated for 2 min. Subsequently, the samples were sonicated three times on ice using a high intensity ultrasonic processor (Scientz-1200E, Hangzhou, China). The residual impurity was removed by centrifugation at 16,000× g for 10 min at 4 °C. Finally, proteins were precipitated with cold 15% trichloroacetic acid for 2 h at −20 ° C. After centrifugation for 10 min at 4 °C, and the precipitate was further washed with cold acetone thrice. Protein concentration was quantified using a BCA protein assay kit (Beyotime, Shanghai, China, Table S1). The 15 µg extracted protein was individually separated by 10% SDS-PAGE, and the gel protein profile from each sample was presented in Fig. S2 (*Guo et al., 2019*).

A total of 300 µg proteins per sample was used for trypsin digestion. Briefly, each sample was added DTT to 100 mM and incubated for 5 min at 100 °C, followed by cooling and processing with 200 µL UA buffer containing 8M urea and 150 mM TrisHCl (Sigma, Burlington, MA, USA). The supernatant was discarded after centrifugation at 12,000×g for 15 min. The pellet was further processed with 200 µL UA buffer again. After centrifuging, 50 mM iodoacetamide (IAA, Sigma, Burlington, MA, USA) was added to alkylate the solution for 30 min at RT in darkness, followed by centrifugation at 12,000× g for 10 min. 100 µL UA buffer was added and centrifuged again. This step was followed by a buffer exchange with 100 µL of NH_4HCO_3 buffer and further centrifugation at 14,000× g for 10 min. The digestion process involved incubation with 60 µL of trypsin buffer (6 µg trypsin in 40 µL NH_4HCO_3 buffer) for 16–18 h at 37 °C.

TMT labeling and fractionation of peptides

After trypsin digestion, peptides were initially desalted by Strata X C18 SPE column (Phenomenex, Signa, Innsbruck, Austria), and subsequently dried by vacuum centrifugation. The peptides (100 µg) from each sample were added to 0.5 M TEAB solution and processed using the 10-plex TMT kit (Thermo Fisher Scientific, Waltham, MA, USA). Briefly, the above peptides dissolved solution was incubated with the TMT regent (1 unit of labeling reagent was used for 100 µg of peptide), which was reconstituted in 24 µL anhydrous acetonitrile (CAN) for 2 h at RT. Then, four pooled fractions of C group have been labeled with 126 (C1), 127N (C2), 127C (C3) and 128N (C4) tags, while four pooled fractions of B group have been labeled with 128C (B1), 129N (B2), 129C (B3) and 130N (B4) tags, respectively. The reaction was stopped with 8% ammonium hydroxide. Differently labeled peptides were mixed equally, desalted and vacuum dried (*Huang et al., 2017*; *Muraoka et al., 2019*), then fractionation into fraction using high pH reverse-phase column from Pierce™ high pH reversed-phase peptide fractionation kit (Thermo Fisher Scientific, Waltham, MA, USA) according to the manufacturer's protocol. The peptides finally were combined into 10 fractions and dried by vacuum centrifugation.

LC-MS/MS analysis

The peptides were loaded onto a Trap Column (100 µm ×20 mm, 5 µm, C18, Dr. Maisch GmbH) using 0.1% (v/v) solvent A (formic acid, FA). Separation was then performed on a chromatographic column (75 µm ×150mm, 3 µm, C18, Dr. Maisch GmbH) using an increase of solvent B (0.1% FA in 95% acetonitrile solution). The increasing profile was setting as follows: an increase from 2% to 8% for 2 min, 8% to 28% for 69 min, 28% to 40% for 8 min, then a rise to 100% for 2 min, and sustained at 100% for an additional 9 min, overall process was conducted at a constant flow rate of 300 nL/min on an EASY-nLC 1200 UPLC system (Thermo Fisher Scientific, Waltham, MA, USA). Then, mass spectrometry (MS) analysis was performed by a Q Exactive HF-X mass spectrometer (Thermo Fisher Scientific, Waltham, MA, USA) in the positive ion model and data-dependent acquisition for 90 min. A full scan range of MS was set to 350–1,800 m/z at a resolution of 60,000@m/z 200. Automatic gain control (AGC) target was set at 3E6 ions and the maximum injection time was set at 50 ms. Afterwards, MS/MS was performed in the same order. The setting parameters as following: resolution of MS2 scan was 45,000@m/z 200, AGC target was 1E5,

the maximum injection time was 50 ms, activation type was higher energy dissociation (HCD), isolation window was 1.2 m/z, and normalized collision energy was set as 32.

Identification and quantification of proteins

A Proteome Discoverer 2.4 software (v.1.6.0.16) was used to retrieve and analyze the LC-MS/MS raw data. Specified search parameters were as follows: (1) a target-reverse database derived from https://www.uniprot.org/taxonomy/9925 protein database: Uniprot_Capra hircus (goat)_9925 (35,503 sequences).fasta; (2) quantitation type: TMT 10-plex isobaric labels; (3) mass tolerance: precursor ions tolerance: 10 ppm, and mass error tolerance of fragment ions: 0.02 Da; (4) digestion: trypsin/P; (5) modifications: fixed modifications: Carbamidomethyl (C), TMT6plex (K), TMT6plex (peptide N-term), and variable modifications: oxidation (M), acety (protein N-term); (6) FDR setting: $\leq$ 1%; (7) unique peptides per protein setting: $\geq$ 1.

Bioinformatic analysis

Bioinformatics data were carried out using Perseus software (v.1.6.5.0), microsoft excel (v.2010) and R statistical computing software (v.4.0.5). Differentially significant abundant proteins (DAPs) were screened base on a fold change (FC) cutoff of >1.20 or <0.833, and P-value < 0.05. Protein abundance data were grouped together *via* hierarchical clustering. Information of sequence annotation was extracted from UniProtKB/Swiss-Prot, Gene Ontology (GO) and Kyoto Encyclopedia of Genes and Genomes (KEGG). GO and KEGG enrichment analyses were carried out with the Fisher's exact test, and FDR correction for multiple testing was also performed. Annotation informations of GO function were obtained from the UniProt-GOA database (http://www.ebi.ac.uk/GOA/) combined with Inter-ProScan tool (https://www.ebi.ac.uk/interpro/), which including three categories: biological process (BP), cellular component (CC) and molecular function (MF). The KASS service (https://www.genome.jp/tools/kaas/) combined with DAVID tool (https://david.ncifcrf.gov/) were performed to annotate proteins' KEGG informations (*Guan et al., 2021*). The enrichment analysis of GO and KEGG pathway with P-value < 0.05 was considered statistically significant. WoLF PSORT service (https://www.genscript.com/wolf-psort.html) was used to predict protein subcellular localization. String database (http://www.string-db.org/) combined with cytoscape software (v.3.9.1) were used for constructing protein-protein interaction (PPI) networks.

Parallel reaction monitoring quantification

Quantification verification of sperm samples was performed using parallel reaction monitoring (PRM) assay, protocols of sperm samples preparation, total protein extraction and trypsin digestion were the same as the TMT LC-MS/MS procedure. A total of 2 µg peptides of each sample were analyzed using an Easy-nLC 1200 UPLC system (Thermo Fisher Scientific, Waltham, MA, USA). Afterwards, MS/MS analysis was further performed in a Q Exactive HF-X mass spectrometer (Thermo Fisher Scientific, Waltham, MA, USA). Running parameters of the mass spectrometer were set as follows: (1) analysis duration was 60 min in positive ion detection mode. (2) precursor ion scan range of MS was 300–1,200 m/z at a resolution of 60,000@m/z 200. (3) AGC target was 3E6 ions, and the maximum

Table 1 Effects of BHT on the motility and motile parameters of post-thaw goat sperm.

Groups		TM (%)	PM (%)	VCL (μm/s)	VAP (μm/s)	VSL (μm/s)	ALH (μm)	BCF (Hz)
C		53.05 ± 3.84[a]	29.22 ± 2.06[a]	79.31 ± 4.32[a]	55.75 ± 0.84[a]	48.54 ± 2.94[a]	2.77 ± 0.15[a]	6.93 ± 0.52[a]
B (mM)	0.5	61.68 ± 0.58[b]	39.22 ± 2.98[b]	82.50 ± 4.47[a]	64.97 ± 1.15[b]	53.79 ± 0.68[a]	2.97 ± 0.15[a]	7.64 ± 0.35[a]
	1.0	54.14 ± 2.33[ab]	33.91 ± 1.71[ab]	83.04 ± 2.10[a]	63.38 ± 3.95[ab]	51.65 ± 3.29[a]	2.71 ± 0.18[a]	6.97 ± 0.31[a]
	2.0	51.98 ± 3.02[a]	33.02 ± 2.61[ab]	82.25 ± 3.76[a]	61.10 ± 3.76[ab]	48.70 ± 2.80[a]	2.72 ± 0.15[a]	7.35 ± 0.43[a]

Notes.
Within the same column, values with different lowercase superscripts differ significantly ($P < 0.05$).

injection time (MIT) was 50 ms. Followed by performing the same order during MS2, and the setting parameters as following: resolution of MS2 scan was 30,000@m/z 200, AGC target was 1E6, the MIT was 100 ms, activation type was HCD, isolation window was 1.6 m/z, and normalized collision energy was 28. Raw data of PRM-MS/MS were searched through the MaxQuant search engine, following processing using Skyline (v.4.1) (*Zhang et al., 2022*).

Statistical analysis

IBM SPSS26.0 software (SPSS Inc., Chicago, IL, USA) was used to distinguish differential data. Based on equal variance assumption, check of variance homogeneity and the multiple comparison analysis by Duncan's test were conducted. Prism software (GraphPad, v.6.07) was used to present graphs as means ± standard error of the mean (S.E.M). A two-tailed Fisher's exact test with Bonferroni correction (*P*-value < 0.05) was employed to test the enrichment of DAPs. Functional enrichment with an adjusted *P*-value < 0.05 was considered significant.

RESULTS

Effects of BHT on sperm quality-associated parameters

Result of the motility and motile parameters in goat sperm were shown in Table 1. Sperm in samples frozen with 0.5 mM BHT showed significantly higher total motility (61.68 ± 0.58%) and progressive motility (39.22 ± 2.98%) than control samples (53.05 ± 3.84% and 29.22 ± 2.06%, respectively) (*P* = 0.044 and *P* = 0.012). Concurrently, sperm in samples frozen with 0.5 mM BHT showed significantly higher average velocity (VAP, μm/s) than the control (*P* = 0.039). However, other motile parameters of post-thaw sperm such as curvilinear velocity (VCL, μm/s), rectilinear velocity (VSL, μm/s), sway amplitude (ALH, μm) and whip frequency (BCF, Hz) showed no differences among 0.5 mM, 1.0 mM, 2.0 mM BHT and the control groups (*P* > 0.05).

Additionally, post-thaw sperm in samples frozen with 0.5 mM BHT showed extremely significantly higher levels of plasma membrane integrity (PMI, %) than the control samples (*P* = 0.001), whereas, there were no difference among 1.0 mM, 2.0 mM BHT-treated and the control groups (Fig. 1A). Similarly, acrosome integrity (ACRI, %) of post-thaw sperm showed the best in 0.5 mM BHT-replenished group as compared to other groups (Fig. 1B). Supplement of 0.5 mM, 1.0 mM and 2.0 mM BHT to cryomedium can reduce ROS content (%) in post-thaw sperm, respectively; thereinto, only the 0.5 mM treated group
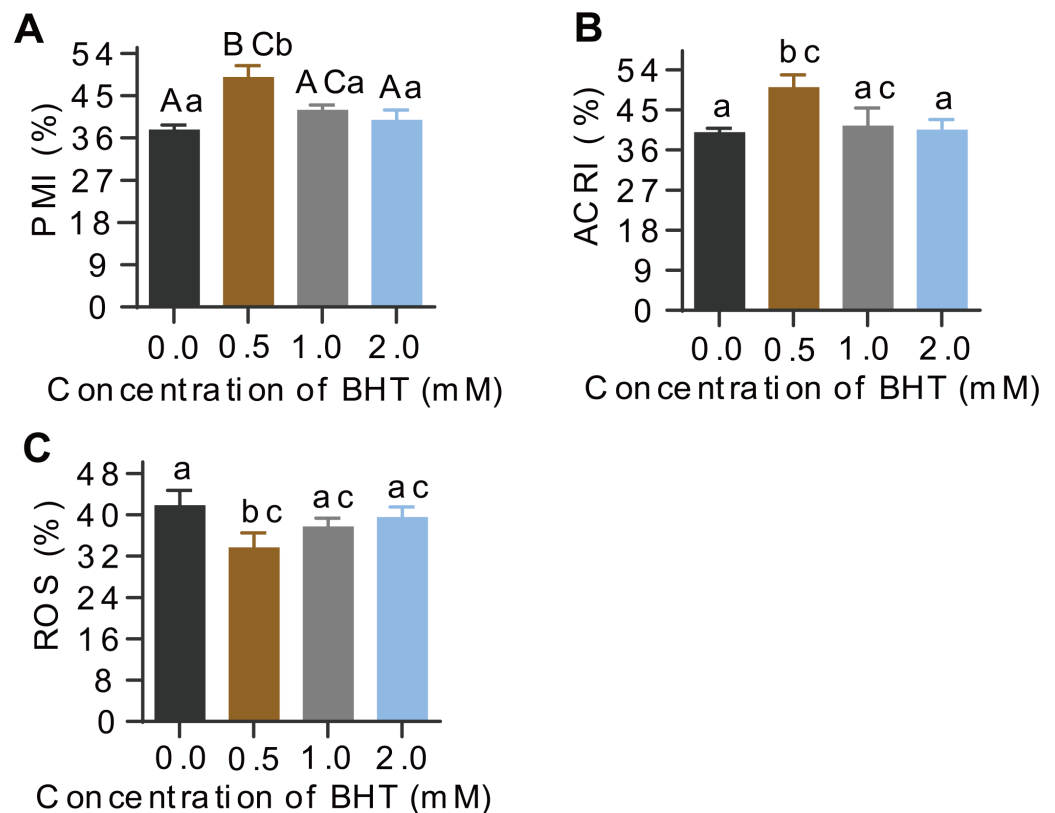
Figure 1 **Effects of BHT on levels of PMI%, ACRI% and ROS of post-thaw goat sperm.** Values with different lowercase superscripts differ significantly ($P < 0.05$) and different uppercase superscripts differ significantly extremely ($P < 0.01$).

Full-size ⊡ DOI: 10.7717/peerj.17580/fig-1

presented significantly reduced sperm ROS content ($P = 0.04$) compared to the control group (Fig. 1C). Raw data of this sperm quality-associated indices were shown in Table S2.

Statistical analysis of MS data

To further explore the underlying molecular effects of 0.5 mM BHT on cryopreserved goat sperm, TMT-based proteomic experiments were performed. Using rigorous statistical filtering, a total of 21,511 unique peptides were identified from 561,255 MS/MS spectrums, with 2,479 corresponding proteins in two groups, of which, 2,476 proteins were quantified (Fig. 2, Table S3).

Identification of DAPs

According to the screening criteria group ratio (fold change >1.2 or <0.833, $P < 0.05$), fold change of DAPs between the comparable groups (C *vs.* B) was calculated. These DAPs were effectively separated using RStudio (version 3.6.3), as shown in the volcano plot (Fig. 3A), overall, 17 DAPs were identified, where 3 and 14 proteins were highly expressed abundance in C and B groups, respectively (Fig. 3B). All DAPs of goat spermatozoa in C compared to B groups were given in Table 2. Among these, the characterized protein GST class-pi appeared the highest relative up regulation and the 14-3-3 protein theta showed the
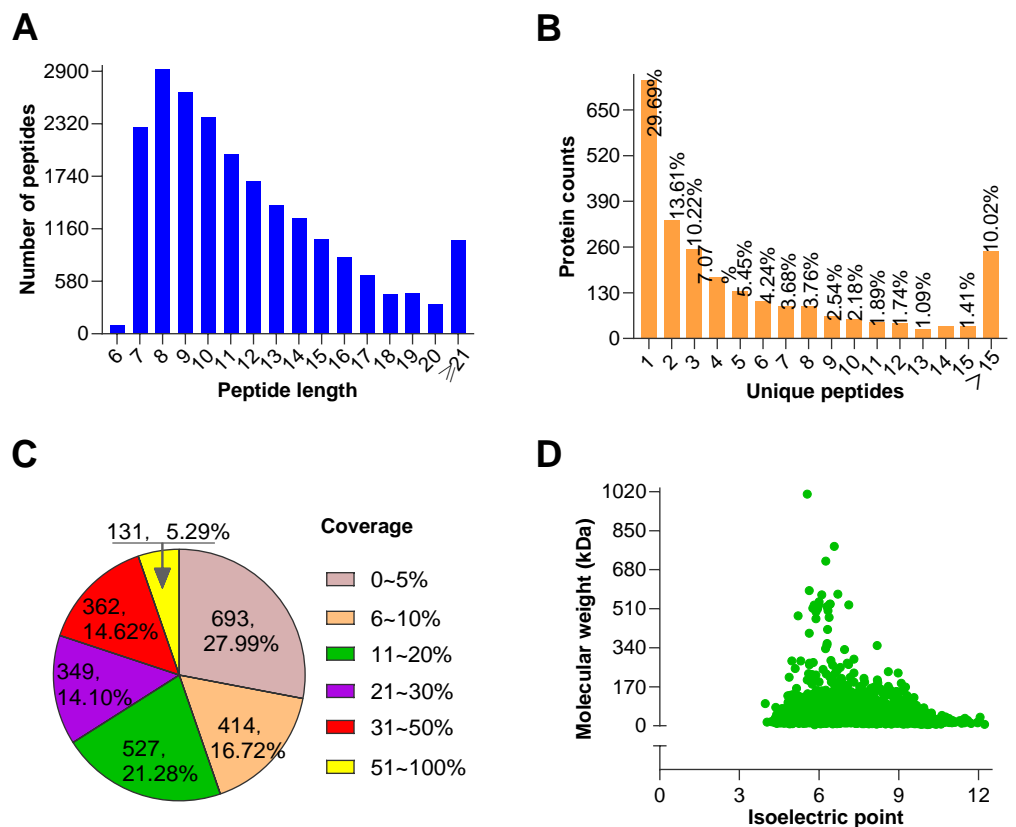
Figure 2 **Quality control results of proteins.** (A) Distribution of peptide number and length, the abscissa represents the peptide length, and the ordinate represents the number of multiple peptides corresponding to the length. (B) Distribution of unique peptide corresponding to protein, the abscissa represents unique peptide number, and the ordinate represents protein counts corresponding to the unique peptide. (C) Protein coverage (it is defined as a ratio of all unique peptides' length sum to total length of the protein, and is only a reference value related to protein confidence), most proteins coverages were under 30%. (D) Distribution of protein molecular weight and isoelectric point, the abscissa represents isoelectric point of the quantified protein, and the ordinate represents molecular weight of the quantified protein. A large molecular weight range indicates a wide range of quantified proteins.

Full-size 🖼 DOI: 10.7717/peerj.17580/fig-2

highest relative down regulation between the comparable groups. These DAPs were mainly distributed in the plasma membrane (23.53%) and unknown subcellular sites (23.53%), followed by cytoplasm (17.65%) and acrosome (11.77%) based on web-server named Euk-mPLoc 2.0 (Fig. 3C).

PRM quantification

For more authentication of TMT LC-MS/MS proteomic data, we performed PRM verification. Here, the peptide information used to PRM quantification is shown in Table S4, and nine target DAPs with the changed over 1.20 fold and at least two unique peptides for validation, namely, KRT4, KRT5, KRT79, KRT1, ACE, KRT14, SLLP1, KRT3 and IQCF1. Among them, KRT4, KRT5, KRT79, KRT1, ACE, KRT14, KRT3 and IQCF1 were downregulated (C/B ratio < 0.833), whereas, the expression of SLLP1 was upregulated
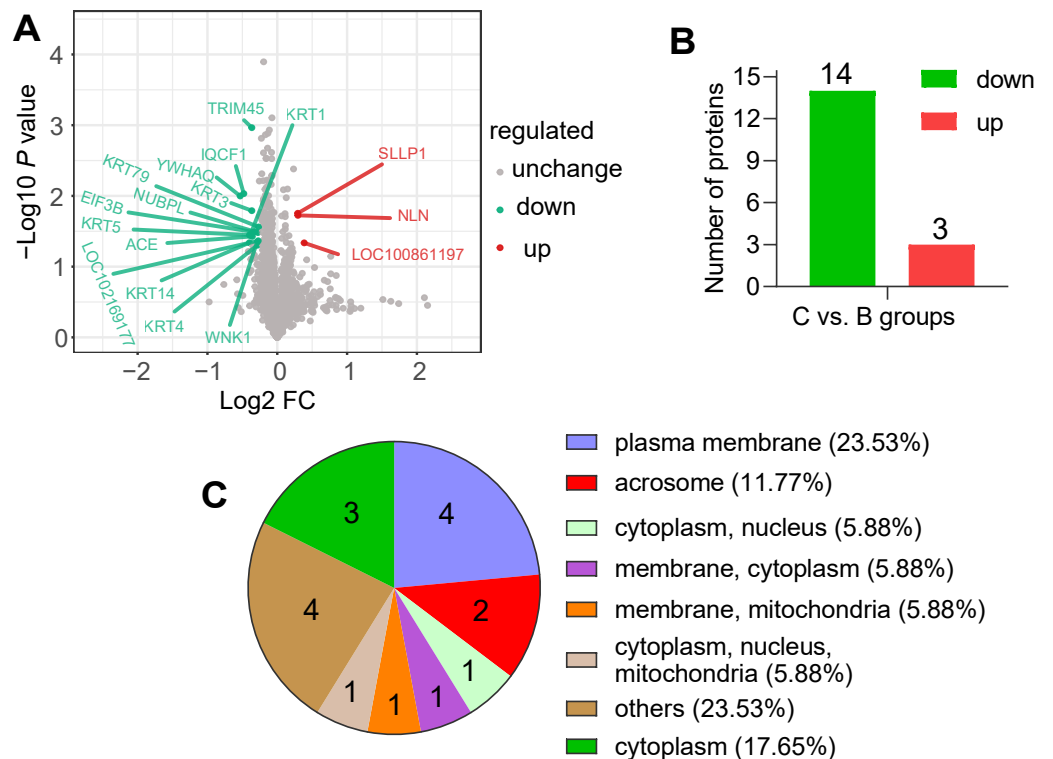
Figure 3 Screening of the DAPs. (A) Volcano plots of the comparison (C vs. B). The horizontal coordinate represents the fold change of the DAPs (log2). The vertical coordinate represents the P-value (10 is the logarithmic transformation at the bottom). Red points indicate significantly upregulated DAPs; green points indicate significantly downregulated DAPs, and gray points indicate proteins that weren't differential abundance. (B) Counts of DAPs. (C) Subcellular localization of DAPs.

Full-size 🖼 DOI: 10.7717/peerj.17580/fig-3

(C/B ratio > 1.20) (Fig. 4). The PRM results showed a similar trend to the TMT results, which indicated that the proteomics data were reliable.

Functional enrichment analysis based on DAPs

To explore the potential roles of DAPs in the comparable group (C/B), we conducted GO terms and KEGG pathway. DAPs were clustered into 11 GO classes, which contains biological process (BP), cellular component (CC) and molecular function (MF), each DAP was assigned more than one term. Concerning the BP, DAPs were associated with metabolic process, multi-organism process, reproduction, reproductive process, and cellular process; while their enrichment categories included translation regulator activity, structural molecule activity, catalytic activity, and binding in CC terms; and these DAPs were involved in cellular anatomical entity and protein-containing complex in MF terms (Fig. 5A, Table S5). KEGG was utilized for functional pathway annotation of DAPs, there proteins were mapped to the pathways such as renin-angiotensin system and glutathione metabolism pathways (Fig. 5B, Table S6). Additionally, DAPs underwent a protein-protein interaction (PPI) network in the String database (v.11.5, https://cn.string-db.org/). Notably, KRTs family such as KRT1, KRT3, KRT4, KRT5, KRT14 and KRT79 act "cross-talk" nodes

Table 2 The proteins that were differentially abundant in comparable groups (C vs. B).

Accession	Description	Gene name	MW [kDa]	Score	Coverage [%]	Unique eptide	P- value	FC
A0A452DMF8	Keratin 5	KRT5	60.2	95.13	31	12	0.036	0.760
A0A452DT87	Nucleotide binding protein like	NUBPL	34.8	2.64	3	1	0.032	0.801
A0A452DXG9	Zinc finger protein 474	LOC102169177	52.1	2.37	2	1	0.043	0.827
A0A452E278	Eukaryotic translation initiation factor 3 subunit B	EIF3B	89.3	2.50	1	1	0.033	0.825
A0A452EAT2	Angiotensin-converting enzyme	ACE	150.5	159.73	17	24	0.037	0.781
A0A452EB32	IQ motif containing F1	IQCF1	23.5	56.42	33	6	0.009	0.717
A0A452EBB3	Non-specific serine/threonine protein kinase	WNK1	246	2.65	0	1	0.046	0.817
A0A452ECX7	14-3-3 protein theta	YWHAQ	27.7	32.54	23	1	0.0100	0.692
A0A452EJW7	GST class-pi	LOC100861197	23.7	8.06	15	2	0.046	1.306
A0A452EN33	Keratin 14	KRT14	55.9	67.02	23	4	0.046	0.758
A0A452ENV4	Keratin 79	KRT79	57.8	28.53	11	1	0.027	0.831
A0A452F5B0	Tripartite motif containing 45	TRIM45	63.6	3.52	1	1	0.001	0.777
A0A452FN18	Keratin 3	KRT3	64.2	77.34	15	3	0.016	0.777
A0A452FYR1	Neurolysin	NLN	80.4	3.82	3	2	0.019	1.228
A0A452G885	Keratin 4	KRT4	55.9	138.89	37	13	0.049	0.820
A0A452GA47	Cytokeratin-1	KRT1	63.6	73.50	11	4	0.036	0.765
D7R6C7	Sperm acrosome membrane-associated protein 3	SLLP1	18	49.33	31	5	0.018	1.226

in the functional modules. They played roles as key intermediate filament proteins that interact with various regulatory proteins, aimed to initiate signaling cascades (Fig. 5C, Table S7).

DISCUSSION

Effects of BHT on post-thaw sperm quality are dose dependent

An imbalance between reactive oxygen species (ROS) and antioxidants in favor of the former, this phenomenon results in progression to oxidative stress in cells and tissues (*Banihani, 2017*). In cryopreserved sperm, excessive levels of ROS generated in mitochondria can mediate lipid peroxidation (LPO) in the plasma membrane, coupled with exhaustion of antioxidants, resulting in oxidative injuries, which induce damage of structural and functional components such as proteins, membrane, and DNA in spermatozoa, finally leading to decrease of sperm motility (*Santiani et al., 2014*; *Mislei et al., 2020*), its subsequent ability to approach an egg and successful internal fertilization (*Merino et al., 2015*; *Hyakutake, Sato & Sugita, 2019*; *Merino et al., 2020*; *Park & Pang, 2021*).

Injury to sperm by free radicals generated during the freezing-thawing process could be minimized by supplement of antioxidative protectants in conventional cryo-media, reducing oxidative stress, concurrently, enhancing the motility and membrane integrity while decreased the LPO in sperm (*Thuwanut et al., 2008*; *Gharagozloo & Aitken, 2011*; *Merino et al., 2020*). As a promising antioxidant, BHT has been discussed exclusively in nearly six thousand publications (*Yehye et al., 2015*). Thus far, this lipid-soluble phenolic compound has been confirmed positive effects on cryopreserved sperm (*Jara et al., 2019*; *De*
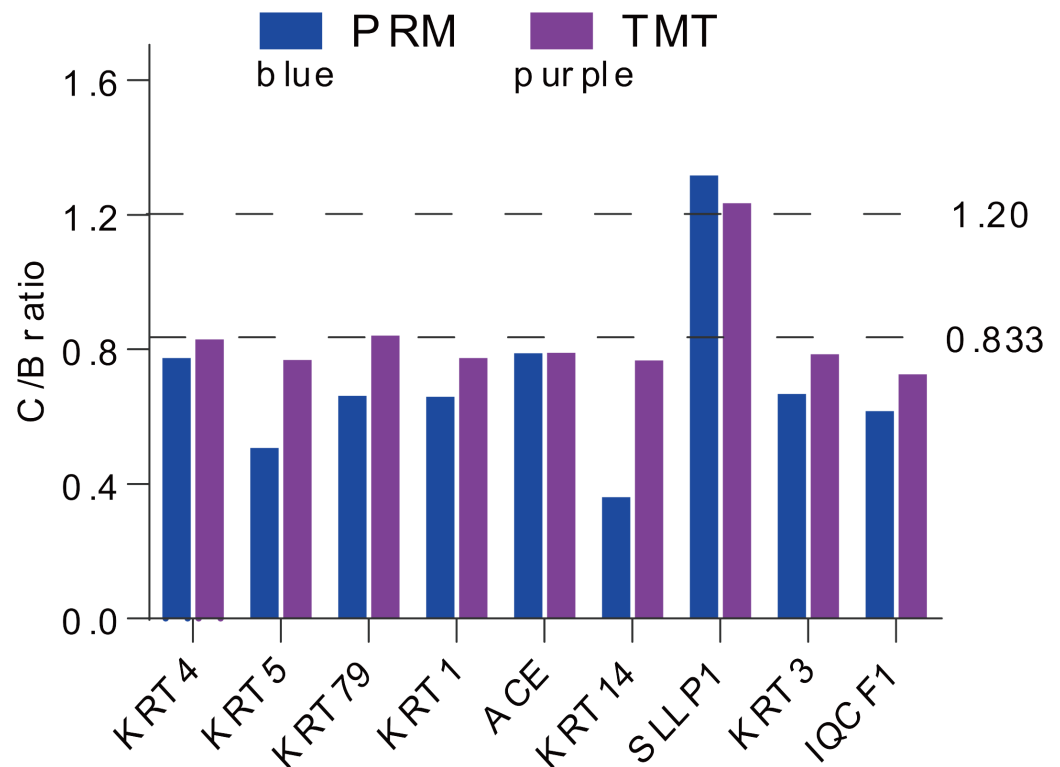
Figure 4 **Expression patterns of selected DAPs using TMT analysis and PRM validation.** From top to bottom, two dotted lines represent 1.20-fold (up-regulation) and 0.833-fold (down-regulation), respectively.

Full-size ▣ DOI: 10.7717/peerj.17580/fig-4

Andrade et al., 2023). Specifically, BHT readily penetrate the sperm membrane, enhancing its fluidity and influencing the membrane phase transition. This action potentially prevents ice-crystal formation within sperm cell (*Hammerstedt et al., 1976*; *Khumran et al., 2015*). Additionally, penetrated BHT also acts primarily as a proton donor for the free radicals and the regenerate acylglycerol molecule, or it can reduce sites suitable for molecular oxygen attack, and terminate oxidation of the free-radical chain reaction, thereby decreasing the harmful effects of ROS on sperm during freezing/thawing process (*Fujisawa, Kadoma & Yokoe, 2004*; *Osipova et al., 2016*; *Fasihnia et al., 2020*). There are available references on the effects of BHT added to semen freezing extenders to protect sperm during cryopreservation in a dose dependent manner. For example, addition of 0.5 mM and 1.0 mM BHT appears to be optimal for the cryopreservation of human semen, due to its antioxidant property for improving the progressive sperm motility and reducing ROS production compared to the control (*Ghorbani et al., 2015*; *Merino et al., 2015*). In canine, supplementation of 0.2–0.8 mM BHT in the cryo-media did not affect the cryopreserved sperm motility, viability and acrosome integrity whilst 1 mM or 1.5 mM BHT significantly improves sperm plasma membrane (*Neagu et al., 2010*; *Sun et al., 2020*). Additionally, higher values of the sperm motility, average path velocity, GPx activity, and acrosome integrity in the cryo-medium supplement of 1.5 mM BHT than those in the control (*Neagu et al., 2010*). However, these
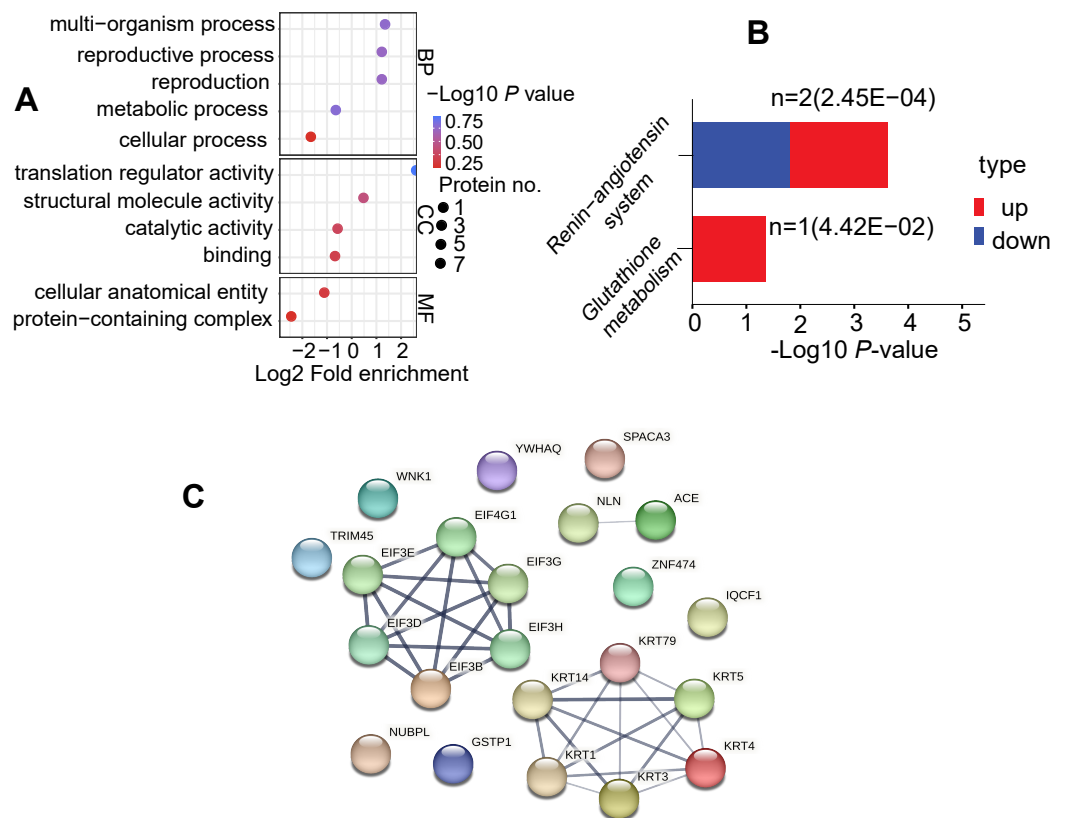
Figure 5 Functional enrichment analysis of DAPs. (A) GO analysis for DAPs. Three functional domains were displayed that including biological process, cellular component and molecular function terms. (B) Analysis of KEGG pathways in the comparable group (C *vs*. B). (C) Protein-protein interaction network diagram of DAPs

Full-size 🖼 DOI: 10.7717/peerj.17580/fig-5

characteristics of chilled sperm reversed when BHT concentration reached 1.6 mM in the extender (*Sahashi et al., 2011*). In Murrah buffalo bull, 0.5–1.0 mM BHT-supplementation in freezing extenders significantly increased the progressive motility, viability, and acrosome integrity of frozen thawed spermatozoa compared to the control (*Nain et al., 2022*). Expansively, 0.5–2.0 mM BHT-supplementation in extenders significantly decreased lipid peroxidation of cryopreserved boar sperm in relation to the control, thereinto, motility, membrane and acrosome integrities, fertilizing ability of post-thaw sperm were the highest by addition of 1.0 mM BHT (*Trzcinska et al., 2015*). Nevertheless, our study showed that 0.5 mM BHT-supplementation in semen extender was the optimal concentration for improving the motility (TM, PM), plasma membrane and acrosome integrities, and decreasing levels of ROS in cryopreserved goat sperm compared to the control, which effectively improved the quality of frozen sperm.

BHT modifies the protein profile of goat sperm during cryopreservation

The TMT based quantitative proteomic technique was applied to evaluate effects of BHT on the proteome of cryopreserved spermatozoa in Yunshang black goats. After bioinformatics analysis, overall, 17 DAPs involved in sperm characteristics and functions were screened between C and B groups. Those proteins were mainly involved in sperm-egg binding and fertilization, RNA transport, estrogen signaling, structural molecule activity and glutathione metabolism *etc.*, which may be associated with the decline of sperm quality after cryopreservation, and the molecular role of BHT in reversing this adverse state.

For instance, sperm acrosome membrane-associated protein 3 (SLLP1) and GST class-pi (LOC100861197) were more abundant in C group. SLLP1 (also referred to as SPRASA) has been identified firstly in the acrosome of human sperm and involved in immune-mediated infertility (*Chiu et al., 2004*). As a member of c-type lysozyme/alpha-lactalbumin family, SPRASA has an exon-intron organization and sequence conservation, similar to c-type lysozymes (*Chiu et al., 2004*; *Wagner et al., 2015*). Afterwards, it has been reported that the protein could be a target for anti-sperm antibodies in some infertile male, playing possible roles in sperm-egg bonding process, as well as subsequent development of early embryo in hamster, murine or bovine models (*Prendergast et al., 2014*). In this study, the expression of SPRASA was higher in cryopreserved goat spermatozoa without antioxidant cryo-protection, suggesting that this protein may be a potential infertile marker of frozen-thawed goat sperm, and its specific molecular function is worth further exploration. Glutathione-S-transferases (GSTs) have been demonstrated to be present on the goat sperm surface that serve as zinc-responsive antioxidants to bind oocyte (*Aravinda et al., 1995*; *Hemachand & Shaha, 2003*; *Chung, Walker & Hogstrand, 2006*). Remarkably, the isoform of GSTs, namely GST-Pi has recently been shown to be present primarily in sperm plasma membrane and is responsible for binding to the zona pellucida (*Kumar, Singh & Atreja, 2014*). Previous report has been shown that GST-Pi expression in relation to oxidative stress and GST activity (*Huang et al., 2004*). In goat cryopreserved sperm, GST-Pi was up-regulated and the higher levels of oxidative stress, which suggesting that GST-pi expression in sperm with higher levels of oxidative stress may not be enough to eliminate the harmful effects of ROS.

On the contrary, keratins (KRT1, KRT3, KRT4, KRT5, KRT14, KRT79), IQ motif containing F1 (IQCF1), nucleotide-binding protein like (NUBPL), and angiotensin-converting enzyme (ACE) were more abundant in B group than in C group. Interestingly, Keratins are typical intermediate filament proteins, play roles in protecting cell/tissue from stress, and act as biomarkers for some organ diseases (*Moll, Divo & Langbein, 2008*; *Mun, Hur & Ku, 2022*). Here, we identified up-regulated keratins proteins KRT1, KRT3, KRT4, KRT5, KRT14 and KRT79 in cryopreserved goat sperm which treated with a freezing medium containing BHT antioxidant. These keratins as rope-like structures may be involved in microtubules or tension-bearing role in sperm flagella to maintain sperm motility (*Kierszenbaum, 2002*; *Hinsch et al., 2003*).

As a novel acrosomal protein, IQCF1 is proved to interact with calmodulin on the sperm head and functioned in sperm motility, additionally, this protein is associated with sperm

capacitation, especially sperm protein tyrosine phosphorylation and the membrane fusion events during acrosome reaction (*Bendahmane, Lynch & Tulsiani, 2001*; *Fang et al., 2015*). Although it is tempting to hypothesize that IQCF1 expression is correlated with sperm capacitation, more studies are warranted to confirm this finding.

NUBPL is one of the essential subunits for sperm mitochondrial complex I (MCI) assembly, typically, activity of MCI effectively maintains the optimal levels of ROS (*Chai et al., 2017*; *Cheng et al., 2022*), we thereby concluded the indirect effect of NUBPL on ROS production.

For ACE, which has two isoforms, thereinto, the testicular isoform of ACE (tACE) is expressed in haploid elongating spermatids and sperm. Of note, tACE plays an important role in sperm fertilization because of its dual activities of dipeptidase and a GPI-anchored protein releasing factor, and correct positioning and distribution in the sperm membrane is prerequisite for the fertility (*Sibony, Segretain & Gasc, 1994*; *Deguchi et al., 2007*; *Pencheva et al., 2021*). *Ojaghi et al. (2018)* suggested that freezing and thawing process could reduce the abundance level and activity of tACE in bull sperm. Our finding of tACE has a significant increase in the expression level in highly motile goat cryopreserved sperm which being storage in cryomedium contains BHT. Therefore, we may conclude that tACE indeed associates with sperm fertilization competence, it could serve as marker for fertilizing ability of spermatozoa.

CONCLUSIONS

The utilization of antioxidants during cryopreservation has emerged as a promising approach to mitigate detrimental effects of ROS on sperm quality. Our study has underscored the significant enhancement in goat sperm quality parameters after freezing/thawing, when the extender was supplemented with 0.5 mM of BHT. Furthermore, the over-expression of certain proteins, such as SLLP1, GST-Pi, IQCF1, NUBPL and tACE were observed, suggesting their potential as novel biomarkers for appraising post-thaw sperm quality and fertility in the goat. As the field advances, a deeper understanding of these proteins and their interaction with antioxidants like BHT will be crucial for refining cryopreservation protocols and enhancing the success rates of AI in goats.

ADDITIONAL INFORMATION AND DECLARATIONS

Competing Interests

The authors declare there are no competing interests.

Author Contributions

- Chunyan Li conceived and designed the experiments, performed the experiments, analyzed the data, prepared figures and/or tables, authored or reviewed drafts of the article, conceptualized the study, and approved the final draft.
- Larbi Allai performed the experiments, analyzed the data, prepared figures and/or tables, authored or reviewed drafts of the article, and approved the final draft.
- Jiachong Liang performed the experiments, prepared figures and/or tables, validated the experiments, and approved the final draft.
- Chunrong Lv performed the experiments, prepared figures and/or tables, validated the experiments, and approved the final draft.
- Xiaoqi Zhao performed the experiments, prepared figures and/or tables, and approved the final draft.
- Xiaojun Ni performed the experiments, prepared figures and/or tables, and approved the final draft.
- Guoquan Wu performed the experiments, prepared figures and/or tables, authored or reviewed drafts of the article, investigated resources, and approved the final draft.
- Weidong Deng performed the experiments, prepared figures and/or tables, analyzed formalization, and approved the final draft.
- Bouabid Badaoui analyzed the data, authored or reviewed drafts of the article, and approved the final draft.
- Guobo Quan analyzed the data, authored or reviewed drafts of the article, and approved the final draft.

Data Availability

The following information was supplied regarding data availability:

The raw data is available at the iProX partner repository: IPX0006546000.

Supplemental Information

Supplemental information for this article can be found online at http://dx.doi.org/10.7717/peerj.17580#supplemental-information.

REFERENCES

Achar JC, Nam G, Jung J, Klammler H, Mohamed MM. 2020. Microbubble ozonation of the antioxidant butylated hydroxytoluene: degradation kinetics and toxicity reduction. *Environmental Research* **186**:109496 DOI 10.1016/j.envres.2020.109496.

Amann RP, Waberski D. 2014. Computer-assisted sperm analysis (CASA): capabilities and potential developments. *Theriogenology* **81(1)**:5–17 DOI 10.1016/j.theriogenology.2013.09.004.

Amidi F, Pazhohan A, Shabani NM, Khodarahmian M, Nekoonam S. 2016. The role of antioxidants in sperm freezing: a review. *Cell Tissue Bank* **17(4)**:745–756 DOI 10.1007/s10561-016-9566-5.

De Andrade A, Balogun K, Machaty Z, Knox RV. 2023. Effects of supplemental antioxidants on in vitro fertility measures for cryopreserved boar spermatozoa. *Theriogenology* **200**:33–42 DOI 10.1016/j.theriogenology.2023.01.025.

Aravinda S, Gopalakrishnan B, Dey CS, Totey SM, Pawshe CH, Salunke D, Kaur K, Shaha C. 1995. A testicular protein important for fertility has glutathione S-transferase activity and is localized extracellularly in the seminiferous tubules. *Journal of Biological Chemistry* **270(26)**:15675–15685 DOI 10.1074/jbc.270.26.15675.

Banihani SA. 2017. Effect of captopril on semen quality. *Andrologia* **49(4)**:e12641 DOI 10.1111/and.12641.

Bendahmane M, Lynch CN, Tulsiani DR. 2001. Calmodulin signals capacitation and triggers the agonist-induced acrosome reaction in mouse spermatozoa. *Archives of Biochemistry and Biophysics* **390(1)**:1–8 DOI 10.1006/abbi.2001.2364.

Chai RR, Chen GW, Shi HJ, WS O, Martin-DeLeon PA, Chen H. 2017. Prohibitin involvement in the generation of mitochondrial superoxide at complex I in human sperm. *Journal of Cellular and Molecular Medicine* **21(1)**:121–129 DOI 10.1111/jcmm.12945.

Chauvin T, Xie F, Liu T, Nicora CD, Yang F, Camp DN, Smith RD, Roberts KP. 2012. A systematic analysis of a deep mouse epididymal sperm proteome. *Biology of Reproduction* **87(6)**:141 DOI 10.1095/biolreprod.112.104208.

Cheng C, Cleak J, Weiss L, Cater H, Stewart M, Wells S, Columbres RC, Shmara A, Morato TC, Zafar F, Schule B, Neumann J, Hatchwell E, Kimonis V. 2022. Early embryonic lethality in complex I associated p.L104P Nubpl mutant mice. *Orphanet Journal of Rare Diseases* **17(1)**:386–397 DOI 10.1186/s13023-022-02446-y.

Chiu WW, Erikson EK, Sole CA, Shelling AN, Chamley LW. 2004. SPRASA, a novel sperm protein involved in immune-mediated infertility. *Human Reproduction* **19(2)**:243–249 DOI 10.1093/humrep/deh050.

Chung MJ, Walker PA, Hogstrand C. 2006. Dietary phenolic antioxidants, caffeic acid and trolox, protect rainbow trout gill cells from nitric oxide-induced apoptosis. *Aquatic Toxicology* **80(4)**:321–328 DOI 10.1016/j.aquatox.2006.09.009.

Deguchi E, Tani T, Watanabe H, Yamada S, Kondoh G. 2007. Dipeptidase-inactivated tACE action in vivo: selective inhibition of sperm-zona pellucida binding in the mouse. *Biology of Reproduction* **77(5)**:794–802 DOI 10.1095/biolreprod.107.060004.

Dutta S, Majzoub A, Agarwal A. 2019. Oxidative stress and sperm function: a systematic review on evaluation and management. *Arab Journal of Urology* **17(2)**:87–97 DOI 10.1080/2090598X.2019.1599624.

Fang P, Xu W, Li D, Zhao X, Dai J, Wang Z, Yan X, Qin M, Zhang Y, Xu C, Wang L, Qiao Z. 2015. A novel acrosomal protein, IQCF1, involved in sperm capacitation and the acrosome reaction. *Andrology* **3(2)**:332–344 DOI 10.1111/andr.296.

Fang Y, Zhao C, Xiang H, Zhao X, Zhong R. 2019. Melatonin inhibits formation of mitochondrial permeability transition pores and improves oxidative phosphorylation of frozen-thawed ram sperm. *Frontiers in Endocrinology* **10**:896 DOI 10.3389/fendo.2019.00896.

Fasihnia SH, Peighambardoust SH, Peighambardoust SJ, Oromiehie A, Soltanzadeh M, Peressini D. 2020. Migration analysis, antioxidant, and mechanical characterization of polypropylene-based active food packaging films loaded with BHA, BHT, and TBHQ. *Journal of Food Science* **85(8)**:2317–2328 DOI 10.1111/1750-3841.15337.

Fujisawa S, Kadoma Y, Yokoe I. 2004. Radical-scavenging activity of butylated hydroxytoluene (BHT) and its metabolites. *Chemistry and Physics of Lipids* **130(2)**:189–195 DOI 10.1016/j.chemphyslip.2004.03.005.

Gharagozloo P, Aitken RJ. 2011. The role of sperm oxidative stress in male infertility and the significance of oral antioxidant therapy. *Human Reproduction* **26(7)**:1628–1640 DOI 10.1093/humrep/der132.

Ghorbani M, Amiri I, Khodadadi I, Fattahi A, Atabakhsh M, Tavilani H. 2015. Influence of BHT inclusion on post-thaw attributes of human semen. *Systems Biology in Reproductive Medicine* **61(1)**:57–61 DOI 10.3109/19396368.2014.968267.

Guan K, Li H, Chen H, Qi X, Wang R, Ma Y. 2021. TMT-based quantitative proteomics analysis reveals the effect of bovine derived MFG-E8 against oxidative stress on rat L6 cells. *Food and Function* **12(16)**:7310–7320 DOI 10.1039/d1fo01135a.

Guo Y, Jiang W, Yu W, Niu X, Liu F, Zhou T, Zhang H, Li Y, Zhu H, Zhou Z, Sha J, Guo X, Chen D. 2019. Proteomics analysis of asthenozoospermia and identification of glucose-6-phosphate isomerase as an important enzyme for sperm motility. *Journal of Proteomics* **208**:103478 DOI 10.1016/j.jprot.2019.103478.

Hammerstedt RH, Amann RP, Rucinsky T, Morse PD, Lepock J, Snipes W, Keith AD. 1976. Use of spin labels and electron spin resonance spectroscopy to characterize membranes of bovine sperm: effect of butylated hydroxytoluene and cold shock. *Biology of Reproduction* **14(4)**:381–397 DOI 10.1095/biolreprod14.4.381.

Hemachand T, Shaha C. 2003. Functional role of sperm surface glutathione S-transferases and extracellular glutathione in the haploid spermatozoa under oxidative stress. *Febs Letters* **538(1-3)**:14–18 DOI 10.1016/s0014-5793(03)00103-0.

Hermo L, Pelletier RM, Cyr DG, Smith CE. 2010. Surfing the wave, cycle, life history, and genes/proteins expressed by testicular germ cells. Part 2: changes in spermatid organelles associated with development of spermatozoa. *Microscopy Research and Technique* **73(4)**:279–319 DOI 10.1002/jemt.20787.

Hinsch E, Boehm JG, Groeger S, Mueller-Schloesser F, Hinsch KD. 2003. Identification of cytokeratins in bovine sperm outer dense fibre fractions. *Reproduction in Domestic Animals* **8(2)**:155–160 DOI 10.1046/j.1439-0531.2003.00408.x.

Huang FK, Zhang G, Lawlor K, Nazarian A, Philip J, Tempst P, Dephoure N, Neubert TA. 2017. Deep coverage of global protein expression and phosphorylation in breast

tumor cell lines using TMT 10-plex isobaric labeling. *Journal of Proteome Research* **16(3)**:1121–1132 DOI 10.1021/acs.jproteome.6b00374.

Huang J, Tan PH, Tan BK, Bay BH. 2004. GST-pi expression correlates with oxidative stress and apoptosis in breast cancer. *Oncology Reports* **12(4)**:921–925 DOI 10.3892/or.12.4.921.

Hyakutake T, Sato K, Sugita K. 2019. Study of bovine sperm motility in shear-thinning viscoelastic fluids. *Journal of Biomechanics* **88**:130–137 DOI 10.1016/j.jbiomech.2019.03.035.

Jara B, Merino O, Sanchez R, Risopatron J. 2019. Positive effect of butylated hydroxytoluene (BHT) on the quality of cryopreserved cat spermatozoa. *Cryobiology* **89**:76–81 DOI 10.1016/j.cryobiol.2019.05.003.

Jia B, Larbi A, Lv C, Liang J, Xiang D, Zhang B, Fang Y, Shen W, Wu G, Quan G. 2022. Identification and validation of ram sperm proteins associated with cryo-injuries caused by the cryopreservation process. *Theriogenology* **184**:191–203 DOI 10.1016/j.theriogenology.2022.03.015.

Jia B, Memon S, Liang J, Lv C, Hong Q, Wu G, Quan G. 2021. Trehalose modifies the protein profile of ram spermatozoa during cryopreservation. *Theriogenology* **171**:21–29 DOI 10.1016/j.theriogenology.2021.05.004.

Khumran AM, Yimer N, Rosnin Y, Ariff MO, Wahid H, Kaka A, Ebrahimi M, Sarsaifi K. 2015. Butylated hydroxytoluene can reduce oxidative stress and improve quality of frozen-thawed bull semen processed in lecithin and egg yolk based extenders. *Animal Reproduction Science* **163**:128–134 DOI 10.1016/j.anireprosci.2015.10.007.

Khumran AM, Yimer N, Rosnina Y, Wahid H, Ariff MO, Homayoun H, Asmatullah K, Bello TK. 2019. Butylated hydroxytoluene protects bull sperm surface protein-P25b in different extenders following cryopreservation. *Veterinary World* **13(4)**:649–654 DOI 10.14202/vetworld.2020.649-654.

Kierszenbaum AL. 2002. Keratins: unraveling the coordinated construction of scaffolds in spermatogenic cells. *Molecular Reproduction and Development* **61(1)**:1–2 DOI 10.1002/mrd.1124.

Kumar R, Singh VK, Atreja SK. 2014. Glutathione-S-transferase: role in buffalo (Bubalus bubalis) sperm capacitation and cryopreservation. *Theriogenology* **81(4)**:587–598 DOI 10.1016/j.theriogenology.2013.11.012.

Leboeuf B, Restall B, Salamon S. 2000. Production and storage of goat semen for artificial insemination. *Animal Reproduction Science* **62(1–3)**:113–141 DOI 10.1016/s0378-4320(00)00156-1.

Li C, Ren C, Chen Y, Wang M, Tang J, Zhang Y, Wang Q, Zhang Z. 2023. Changes on proteomic and metabolomic profiling of cryopreserved sperm effected by melatonin. *Journal of Proteomics* **273**:104791 DOI 10.1016/j.jprot.2022.104791.

Liu T, Han Y, Zhou T, Zhang R, Chen H, Chen S, Zhao H. 2019. Mechanisms of ROS-induced mitochondria-dependent apoptosis underlying liquid storage of goat spermatozoa. *Aging* **11(18)**:7880–7898 DOI 10.18632/aging.102295.

Memon AA, Wahid H, Rosnina Y, Goh YM, Ebrahimi M, Nadia FM, Audrey G. 2011. Effect of butylated hydroxytoluene on cryopreservation of Boer goat semen in tris egg yolk extender. *Animal Reproduction Science* **129**(1–2):44–49 DOI 10.1016/j.anireprosci.2011.10.004.

Merino O, Aguaguina WE, Esponda P, Risopatron J, Isachenko E, Isachenko V, Sanchez R. 2015. Protective effect of butylated hydroxytoluene on sperm function in human spermatozoa cryopreserved by vitrification technique. *Andrologia* **47**(2):186–193 DOI 10.1111/and.12246.

Merino O, Dumorne K, Leidy SV, Figueroa E, Valdebenito I, Farias JG, Risopatron J. 2020. Short-term storage sperm of coho salmon (Oncorhynchus kisutch) at 4 degrees C: effect of sperm: extender dilution ratios and antioxidant butyl-hydroxytoluene (BHT) on sperm function. *Cryobiology* **95**:44–50 DOI 10.1016/j.cryobiol.2020.06.007.

Mislei B, Bucci D, Malama E, Bollwein H, Mari G. 2020. Seasonal changes in ROS concentrations and sperm quality in unfrozen and frozen-thawed stallion semen. *Theriogenology* **144**:89–97 DOI 10.1016/j.theriogenology.2019.12.016.

Moll R, Divo M, Langbein L. 2008. The human keratins: biology and pathology. *Histochemistry and Cell Biology* **129**(6):705–733 DOI 10.1007/s00418-008-0435-6.

Mun J, Hur W, Ku xx. 2022. Roles of keratins in intestine. *International Journal of Molecular Sciences* **23**:14 DOI 10.3390/ijms23148051.

Muraoka S, Jedrychowski MP, Tatebe H, De Leo AM, Ikezu S, Tokuda T, Gygi SP, Stern RA, Ikezu T. 2019. Proteomic profiling of extracellular vesicles isolated from cerebrospinal fluid of former national football league players at risk for chronictraumatic encephalopathy. *Frontiers in Neuroscience* **13**:1059 DOI 10.3389/fnins.2019.01059.

Nain D, Mohanty TK, Dewry RK, Bhakat M, Nath S, Gupta VK, Parray MA. 2022. Butylated hydroxytoluene (bht) improves the post-thaw semen quality in low-dose sperm cryopreservation in murrah buffalo bull. *Cryo Letters* **44**(1):57–65 DOI 10.54680/fr23110110612.

Najafi A, Adutwum E, Yari A, Salehi E, Mikaeili S, Dashtestani F, Abolhassani F, Rashki L, Shiasi S, Asadi E. 2018. Melatonin affects membrane integrity, intracellular reactive oxygen species, Caspase3 activity and AKT phosphorylation in frozen thawed human sperm. *Cell and Tissue Research* **372**(1):149–159 DOI 10.1007/s00441-017-2743-4.

Neagu VR, Garcia BM, Sandoval CS, Rodriguez AM, Ferrusola CO, Fernandez LG, Tapia JA, Pena FJ. 2010. Freezing dog semen in presence of the antioxidant butylated hydroxytoluene improves postthaw sperm membrane integrity. *Theriogenology* **73**(5):645–650 DOI 10.1016/j.theriogenology.2009.10.021.

Ojaghi M, Johnson C, Rizzoto G, Kastelic J, Thundathil JC. 2018. Content and activity of the testis-specific isoform of angiotensin-converting enzyme are reduced in frozen-thawed bull spermatozoa. *Reproduction Fertility and Development* **30**(11):1575–1583 DOI 10.1071/RD17219.

Osipova VP, Berberova NT, Gazzaeva RA, Kudryavtsev KV. 2016. Application of new phenolic antioxidants for cryopreservation of sturgeon sperm. *Cryobiology* **72(2)**:112–118 DOI 10.1016/j.cryobiol.2016.02.006.

Pariz JR, Ranea C, Monteiro R, Evenson DP, Drevet JR, Hallak J. 2019. Melatonin and caffeine supplementation used, respectively, as protective and stimulating agents in the cryopreservation of human sperm improves survival, viability, and motility after thawing compared to traditional test-yolk buffer. *Oxidative Medicine and Cellular Longevity* **2019**:6472945 DOI 10.1155/2019/6472945.

Park YJ, Pang MG. 2021. Mitochondrial functionality in male fertility: from spermatogenesis to fertilization. *Antioxidants* **10(1)**:98 DOI 10.3390/antiox10010098.

Pencheva M, Keskinova D, Rashev P, Koeva Y, Atanassova N. 2021. Localization and distribution of testicular angiotensin I converting enzyme (ACE) in neck and mid-piece of spermatozoa from infertile men in relation to sperm motility. *Cell* **10(12)**:3572 DOI 10.3390/cells10123572.

Peris-Frau P, Martin-Maestro A, Iniesta-Cuerda M, Sanchez-Ajofrin I, Cesari A, Garde JJ, Villar M, Soler AJ. 2020. Cryopreservation of ram sperm alters the dynamic changes associated with in vitro capacitation. *Theriogenology* **145**:100–108 DOI 10.1016/j.theriogenology.2020.01.046.

Pezo F, Yeste M, Zambrano F, Uribe P, Risopatron J, Sanchez R. 2021. Antioxidants and their effect on the oxidative/nitrosative stress of frozen-thawed boar sperm. *Cryobiology* **98**:5–11 DOI 10.1016/j.cryobiol.2020.11.007.

Prendergast D, Woad KJ, Chamley LW, Holland OJ, Shelling AN. 2014. SPACA3 gene variants in a New Zealand cohort of infertile and fertile couples. *Human Fertility* **17(2)**:106–113 DOI 10.3109/14647273.2014.907506.

Ribas-Maynou J, Mateo-Otero Y, Delgado-Bermudez A, Bucci D, Tamanini C, Yeste M, Barranco I. 2021. Role of exogenous antioxidants on the performance and function of pig sperm after preservation in liquid and frozen states: a systematic review. *Theriogenology* **173**:279–294 DOI 10.1016/j.theriogenology.2021.07.023.

Riesco MF, Alvarez M, Anel-Lopez L, Neila-Montero M, Palacin-Martinez C, Montes-Garrido R, Boixo JC, De Paz P, Anel L. 2021. Multiparametric study of antioxidant effect on ram sperm cryopreservation-from field trials to research bench. *Animals* **11(2)**:283 DOI 10.3390/ani11020283.

Ruiz-Diaz S, Grande-Perez S, Arce-Lopez S, Tamargo C, Olegario HC, Perez-Cerezales S. 2020. Changes in the cellular distribution of tyrosine phosphorylation and its relationship with the acrosomal exocytosis and plasma membrane integrity during in vitro capacitation of frozen/thawed bull spermatozoa. *International Journal of Molecular Sciences* **21(8)**:2725 DOI 10.3390/ijms21082725.

Sahashi Y, Otsuki T, Higaki S, Nagano M, Yamashita Y, Hishinuma M. 2011. Effect of butylated hydroxytoluene on dog sperm longevity in chilling storage and cryopreservation. *Journal of Veterinary Medical Science* **73(7)**:895–899 DOI 10.1292/jvms.10-0460.

Santiani A, Evangelista S, Sepulveda N, Risopatron J, Villegas J, Sanchez R. 2014. Addition of superoxide dismutase mimics during cooling process prevents oxidative

stress and improves semen quality parameters in frozen/thawed ram spermatozoa. *Theriogenology* **82(6)**:884–889 DOI 10.1016/j.theriogenology.2014.07.002.

Sibony M, Segretain D, Gasc JM. 1994. Angiotensin-converting enzyme in murine testis: step-specific expression of the germinal isoform during spermiogenesis. *Biology of Reproduction* **50(5)**:1015–1026 DOI 10.1095/biolreprod50.5.1015.

Succu S, Berlinguer F, Pasciu V, Satta V, Leoni GG, Naitana S. 2011. Melatonin protects ram spermatozoa from cryopreservation injuries in a dose-dependent manner. *Journal of Pineal Research* **50(3)**:310–318 DOI 10.1111/j.1600-079X.2010.00843.x.

Sun L, Wu C, Xu J, Zhang S, Dai J, Zhang D. 2020. Addition of butylated hydroxytoluene (BHT) in tris-based extender improves post-thaw quality and motion dynamics of dog spermatozoa. *Cryobiology* **97**:71–75 DOI 10.1016/j.cryobiol.2020.10.006.

Thuwanut P, Chatdarong K, Techakumphu M, Axner E. 2008. The effect of antioxidants on motility, viability, acrosome integrity and dna integrity of frozen-thawed epididymal cat spermatozoa. *Theriogenology* **70(2)**:233–240 DOI 10.1016/j.theriogenology.2008.04.005.

Tiwari S, Dewry RK, Srivastava R, Nath S, Mohanty TK. 2022. Targeted antioxidant delivery modulates mitochondrial functions, ameliorates oxidative stress and preserve sperm quality during cryopreservation. *Theriogenology* **179**:22–31 DOI 10.1016/j.theriogenology.2021.11.013.

Trzcinska M, Bryla M, Gajda B, Gogol P. 2015. Fertility of boar semen cryopreserved in extender supplemented with butylated hydroxytoluene. *Theriogenology* **83(3)**:307–313 DOI 10.1016/j.theriogenology.2014.07.045.

Turk G, Koca RH, Gungor IH, Dayan CS, Acisu TC, Erdem EF, Arkali G, Ozer KS, Kizil M, Sonmez M, Gur S, Yilmaz O, Yuce A, Karatepe M. 2022. Effect of hydrated C (60) fullerene on lipid, vitamin and amino acid composition in frozen-thawed ram semen. *Animal Reproduction Science* **238**:106939 DOI 10.1016/j.anireprosci.2022.106939.

Wagner A, Holland OJ, Tong M, Shelling AN, Chamley LW. 2015. The role of SPRASA in female fertility. *Reproductive Sciences* **22(4)**:452–461 DOI 10.1177/1933719114542009.

Yehye WA, Rahman NA, Ariffin A, Abd HS, Alhadi AA, Kadir FA, Yaeghoobi M. 2015. Understanding the chemistry behind the antioxidant activities of butylated hydroxytoluene (BHT): a review. *European Journal of Medicinal Chemistry* **101**:295–312 DOI 10.1016/j.ejmech.2015.06.026.

Zhang Y, Huang D, Lv N, Zhu G, Peng J, Chou T, Zhu Z, Wang J, Chen Y, Fang X, Qu J, Chen J, Liu S. 2022. Global quantification of glutathione S-transferases in human serum using LC-MS/MS coupled with affinity enrichment. *Journal of Proteome Research* **21(5)**:1311–1320 DOI 10.1021/acs.jproteome.2c00049.

Zhu W, Zhang Y, Ren CH, Cheng X, Chen JH, Ge ZY, Sun ZP, Zhuo X, Sun FF, Chen YL, Jia XJ, Zhang Z. 2020. Identification of proteomic markers for ram spermatozoa motility using a tandem mass tag (TMT) approach. *Journal of Proteomics* **210**:103438 DOI 10.1016/j.jprot.2019.103438.

Zou J, Wei L, Li D, Zhang Y, Wang G, Zhang L, Cao P, Yang S, Li G. 2021. Effect of glutathione on sperm quality in Guanzhong dairy goat sperm during cryopreservation. *Frontiers in Veterinary Science* **8**:771440 DOI 10.3389/fvets.2021.771440.